Semiconductor Plasmonic Nano-cavity Laser on Silicon: Simulation, Design and Fabrication

Qian Wang, Chee Wei Lee, and Kim Peng Lim
Agency for Science, Technology and Research, Data Storage Institute
5 Engineering Drive 1, 117608, Singapore

Abstract— Plasmonic nano-cavity laser based on a III-V semiconductor nano-ring on silicon can operate either in in-plane dipole mode or vertical coaxial mode. This paper gives the simulation, design and some fabrication discussions of this unique nano-cavity laser. Body-of-revolution finite-difference-time-domain (BOR-FDTD) is used for the modal analysis and design of cavity. The spatial and temporal lasing performance of this nano-cavity laser is simulated incorporating the BOR-FDTD with multilevel gain medium model. Comparison between these two lasing modes is presented and numerical analysis shows that the in-plane dipole mode can achieve the smallest mode volume reported so far. Fabrication of this semiconductor plasmonic nano-cavity laser is discussed.This semiconductor plasmonic nano-cavity laser has a deep sub-wavelength foot-print and ultralow power consumption, which can act as an on-chip light source for intrachip data interconnect.

1. INTRODUCTION

On-chip light source with an ultra small footprint and ultralow power consumption is a key device enabling high-speed intra-chip data interconnect. Semiconductor plasmonic nano-cavity has the deep-wavelength light confining capability (overcoming the diffraction limit) and advantages of integration on silicon using heterogeneous III/V on silicon technology and electrically-pumping for practical applications. There are various semiconductor plasmonic laser demonstrated numerically and experimentally so far including Fabry-Perot, nanopatch, nanodisk and coaxial cavity [1–5]. In this paper, a plasmonic III-V semiconductor nano-ring integrated on silicon through an interlayer bonding is considered as shown in Fig. 1.

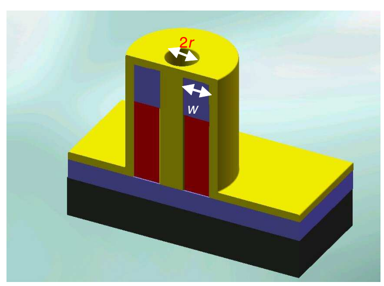

Figure 1: Semiconductor plasmonic nanoring laser.

This plasmonic nanoring cavity can operate at either in-plane dipole mode or vertical co-axial mode. To have a comprehensive analysis and comparison between these two modes, body-of-revolution finite-difference-time-domain is employed for modal analysis and cavity design. The spatial and temporal lasing performance is simulated incorporating the BOR-FDTD with multilevel gain medium model. Comparison between these two lasing modes is presented regarding the resonant wavelength, quality factor and mode profiles. Numerical analysis shows that the in-plane dipole mode laser can achieve the smallest mode volume reported so far. Fabrication of this semiconductor plasmonic nano-cavity laser is discussed and some results are presented.This semiconductor plasmonic nano-cavity laser with a deep sub-wavelength foot-print and ultralow power consumption is promising as an on-chip light source for future intrachip data interconnect.

2. MODELING AND SIMULATION OF THE NANO-RING CAVITY LASER

The nanoring plasmonic laser schematically shown in Fig. 1 requires modeling and simulation in three aspects: 1) semiconductor gain medium; 2) Drude-Lorentz model for the metal and 3) spatial and temporal simulation of electromagnetic field of the nano-cavity using body-of-revolution FDTD.

The Maxwell equation in the format of body of revolution format

$$\begin{cases} \frac{\partial H_{r,o}}{\partial t} = -\frac{1}{\mu}\left(-\frac{\partial E_{\phi,o}}{\partial z} - \frac{1}{r} m E_{z,e}\right) \\ \frac{\partial H_{\phi,e}}{\partial t} = -\frac{1}{\mu}\left(\frac{\partial E_{r,e}}{\partial z} - \frac{\partial E_{z,e}}{\partial r}\right) \\ \frac{\partial H_{z,o}}{\partial t} = -\frac{1}{\mu}\left(\frac{1}{r}\frac{\partial (r E_{\phi,o})}{\partial r} + \frac{1}{r} m E_{r,e}\right) \\ \frac{\partial D_{r,e}}{\partial t} = \left(\frac{1}{r} m H_{z,o} - \frac{\partial}{\partial z} H_{\phi,e}\right) \\ \left(\frac{\partial D_{\phi,o}}{\partial t}\right) = \left(\frac{\partial}{\partial z} H_{r,o} - \frac{\partial}{\partial r} H_{z,o}\right) \\ \frac{\partial}{\partial t} D_{z,e} = \left(-\frac{1}{r} m H_{r,o} + \frac{1}{r}\frac{\partial (r H_{\phi,e})}{\partial r}\right) \end{cases} \tag{1}$$

and $D_{j,e} = \frac{1}{\varepsilon}\sum_{m=1}^{M}\frac{\partial P_m}{\partial t}$ $(j = r, z)$ where P_m is the macroscopic polarization component that links the electromagnetic field with the dynamics of carrier densities for the active gain medium. Detailed formulation of the Drude-Lorentz model and multilevel gain medium model can be found in Ref. [5].

3. NANO-RING CAVITY LASER: IN-PLANE DIPOLE OR COAXIAL LASER?

The nano-ring cavity laser shown in Fig. 1 can operate as an in-plane laser, where the light is confined vertically and resonant cavity is the nano-ring in the horizontal plane. It can also lase

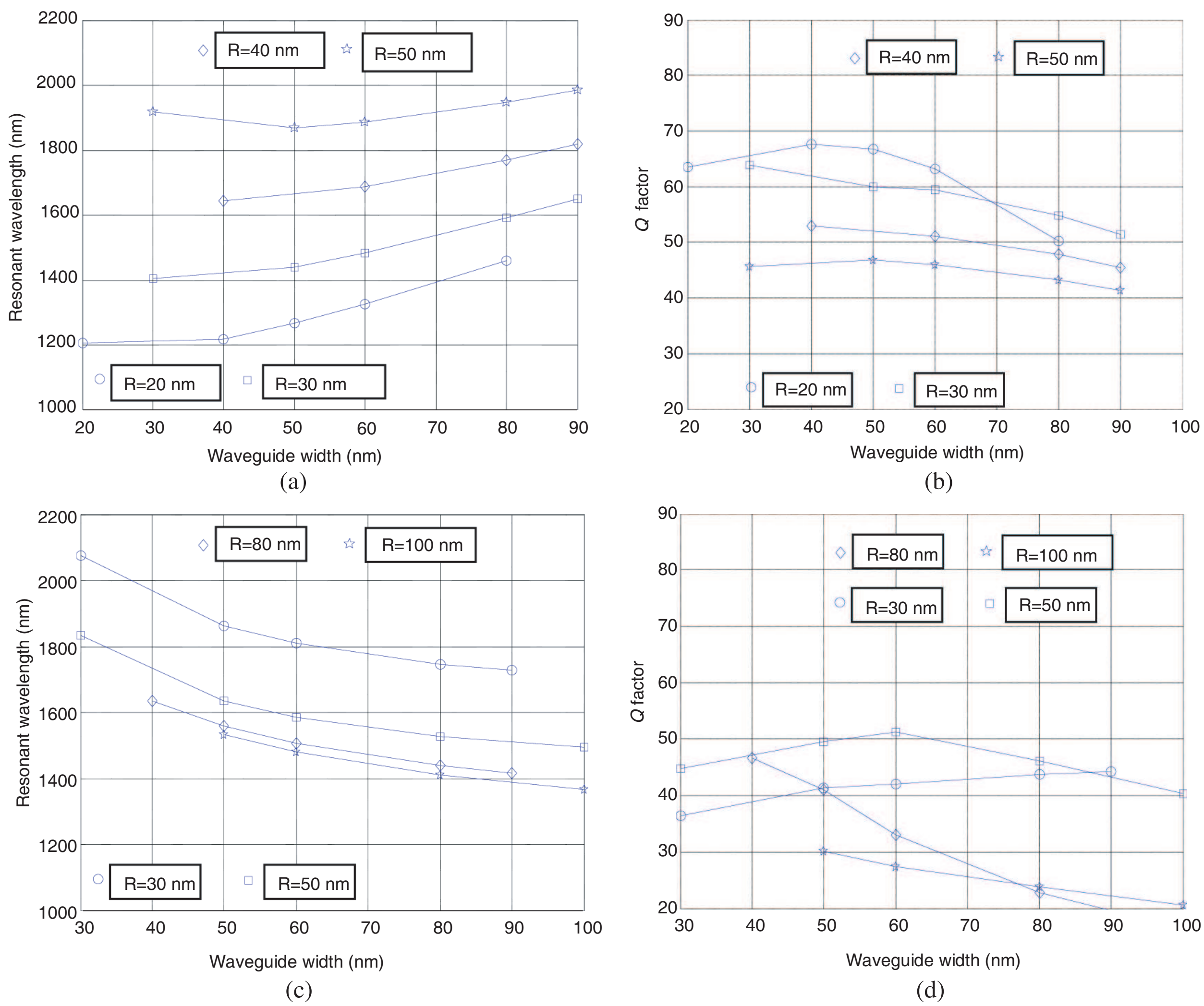

Figure 2: (a) and (b) are resonant wavelengths and Q-factors for nano-ring dipole laser cavity; (c) and (d) are resonant wavelengths and Q-factors for the coaxial laser cavity.

as a coaxial laser as demonstrated in Ref. [4], where the light is confined horizontally as a coaxial plasmonic mode and resonant cavity is formed in the vertical direction. With the above BOR-FDTD, the coaxial lasing mode corresponds to the case of $m = 0$. For the in-plane laser the corresponding $m > 0$ and in this paper $m = 1$ is specifically interested as it refers to in-plane nanoring dipole laser and it can achieve much smaller foot-print as compared to the cases $m > 1$.

As numerical examples, the height of the III-V semiconductor gain region is 200 nm with a refractive index of 3.5 and the material for the top-cladding and interlayer is silicon dioxide. The thickness for the interlayer is 200 nm preventing the leakage for in-plane ring laser and provides sufficient reflectance for coaxial laser. We vary the structure parameters and analyze the influence of these parameters on the device's performance. As representative results, resonant wavelength and quality factors for these two cases are presented in Figs. 2(a)–(d) when varying inner radius R and width of the waveguide W.

As a summary of analysis of both lasing modes: 1) the in-plane laser cavity has a relatively smaller foot print and relatively higher Q factors as compared to the case of coaxial mode when considering the InP material system and operating optical communication wavelength; 2) the coaxial laser cavity is strongly dependent on the thickness of top-cladding and material of interlayer due to the nature of resonant cavity; 3) the in-plane resonant mode has a much smaller mode volume as compared to the coaxial case. In our simulation examples, the in-plane dipole plasmonic laser has an inner radius of 30 nm and width of waveguide of 30 nm, the corresponding mode-volume is only $0.001(\lambda/2n)^3$. For coaxial lasing mode, a cavity with both inner radius and waveguide width of 80 nm gives a close lasing wavelength but the mode volume is $0.014(\lambda/2n)^3$.

Figure 3 shows the intensity profile of the dipole resonant mode (top view) and the corresponding L-L curve simulated with the previous FDTD program with gain medium model.

4. FABRICATION DISCUSSION

The whole device realization consists of three main modules: 1) bonding the InGaAsP gain medium onto silicon substrate through interlayer bonding with thermal SiO_2, which is followed by removing

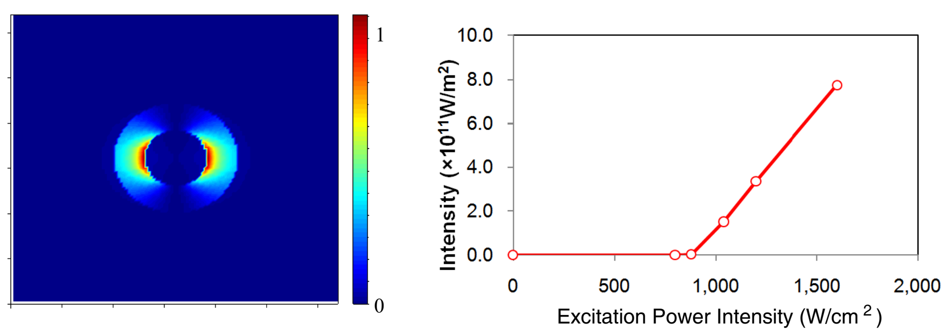

(a) (b)

Figure 3: (a) Intensity profile of the dipole lasing mode; (b) L-L curve simulated by the FDTD program with gain medium model.

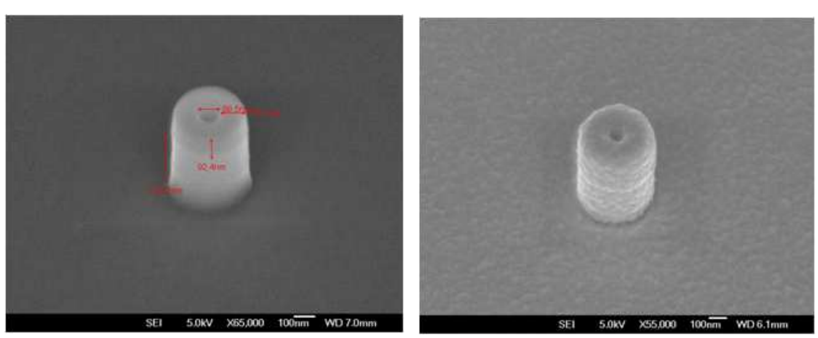

(a) (b)

Figure 4: (a) SEM images of the etched III-V nano-ring cavity; (b) Nanoring cavity coated with silver film.

InP substrate in hydrochloric acid solution; 2) The submicron structures could be defined on the substrate via hydrogen silsesquioxane (HSQ) resist with electron beam lithography, and then directly etched down with chlorine recipe in an inductively coupled plasma reactive-ion-etching system (ICP-RIE) equipped with elevated temperature stage at 250°C; 3) metal film is deposited to form the plasmonic cavity and for the case of in-plane dipole laser, it should be etched back for optical pumping from the top. Figs. 4(a) and (b) are the scanning electronic microscopy images of our III-V etched devices bonded on silicon and coated with metal film. The device prototyping is undergoing.

5. CONCLUSION

This paper has presented the simulation, design analysis and some fabrication discussions of III-V on silicon plasmonic nano-cavity laser. Body-of-revolution finite-difference-time-domain has been used for the modal analysis and design of cavity, which has been also incorporated with the multilevel gain medium model for the spatial and temporal simulation of lasing performance. Comparison between the in-plane dipole laser and vertical coaxial laser has been presented and numerical analysis has shown that the in-plane dipole mode can achieve the smallest mode volume reported so far. Some key fabrication modules of this semiconductor plasmonic nano-cavity laser have been discussed.

REFERENCES

1. Hill, M. T., Y.-S. Oei, B. Smalbrugge, Y. Zhu, T. D. Vries, P. J. V. Veldhoven, F. W. M. V. Otten, T. J. Eijkemans, J. P. Turkiewicz, H. D. Waardt, E. J. Geluk, S.-H. Kwon, Y.-H. Lee, R. N. Tzel, M. K. Smit, “Lasing in metallic-coated nanocavities,” *Nature Photonics*, Vol. 1, 589–594, 2007.
2. Yu, K., A. Lakhani, and M. C. Wu, “Subwavelength metal-optic semiconductor nanopatch lasers,” *Optics Express*, Vol. 18, No. 9, 8790–8799, 2010.
3. Khajavikhan, M., A. Simic, M. Katz, J. H. Lee, B. Slutsky, A. Mizrahi, V. Lomakin, and Y. Fainman, “Thresholdlessnanoscale coaxial lasers,” *Nature*, Vol. 482, 204–207, 2012.
4. Ding, K., M. T. Hill, Z. C. Liu, L. J. Yin, P. J. van Veldhoven, and C. Z. Ning, “Record performance of electrical injection subwavelength metallic-cavity semiconductor lasers at room temperature,” *Optics Express*, Vol. 21, 4728–4733, 2013.
5. Wang, Q. and S.-T. Ho, “A numerical simulation of nanodisk semiconductor-plasmonic laser using BOR-FDTD with a multilevel gain medium model,” *IEEE Photonics Journal*, Vol. 4, 2346–2352, 2012.